CIVIL AND ENVIRONMENTAL ENGINEERING REPORTS

E-ISSN 2450-8594

CEER 2025; 35 (1): 0213-0229
DOI: 10.59440/ceer/200729
Original Research Article

ANALYSIS OF GROUNDWATER TEMPERATURE IN URBAN CONDITIONS - THE CASE OF WROCŁAW, POLAND

Monika HAJNRYCH [1*], Jan BLACHOWSKI [1], Magdalena WORSA-KOZAK [2]
[1] Department of Geodesy and Geoinformatics, Faculty of Geoengineering, Mining and Geology, Wroclaw University of Sciences and Technology, Wroclaw, Poland
[2] Department of Mining, Faculty of Geoengineering, Mining and Geology, Wroclaw University of Sciences and Technology, Wroclaw, Poland

A b s t r a c t

With increasing urbanization, it is becoming important to study the impact of human activity and climate change on the underground environment, including groundwater temperatures. The subsurface urban heat island (SubUHI) is one of the effects of these changes, which consists in increasing the temperature of soil and groundwater in urban areas. This article analyses groundwater temperatures in Wrocław in 2022–2024. The research was conducted at 19 measurement points. The average groundwater temperature was 12.7°C, with values from 8.9°C to 25.4°C. The highest temperatures were recorded in the city center, and the lowest on its western outskirts. Spatial analysis showed higher temperatures in the city center, related to the influence of underground infrastructure and artificial surfaces. At a depth of 15 meters, the influence of external factors on groundwater temperature disappeared. The results indicate the need for further research on local factors influencing groundwater temperature, which may be important for water resource management in cities.

Keywords: SubUHI, spatial interpolation, statistical analysis, urban hydrogeology

1. INTRODUCTION

Today, 55% of the world's population lives in urban areas, a proportion that is expected to increase to 68% by 2050 [1]. The process of urbanisation, combined with climate change affects environmental conditions including the subsurface. Highly urbanized regions depend on abundant and clean groundwater resources for drinking water extraction, and more recently, the urban subsurface has been utilized for low-enthalpy geothermal energy extraction. However, urban areas significantly impact local atmospheric and groundwater environments [2], as human activities can alter the natural physical and chemical conditions of air and groundwater. Among these impacts, the thermal regime of groundwater

[1*] Corresponding author: Monika Hajnrych, Wroclaw University of Sciences and Technology, Faculty of Geoengineering, Mining and Geology, Department of Geodesy and Geoinformatics, Na Grobli Street 15, 50-421 Wroclaw, e-mail: monika.hajnrych@pwr.edu.pl, phone: 71 320 68 79

has become a particularly pressing issue in urban areas, driven by growing concerns about groundwater quality and conservation [3].

One of the documented phenomena in urban areas is the urban heat island (UHI). According to Oke [4,5], there are four types of urban heat island: the boundary-layer urban heat island (BLUHI), canopy UHI (CUHI), surface UHI (SUHI), and subsurface UHI (SubUHI). The last three have been widely studied, whereas the SubUHI phenomenon is the least known and understood mainly due to the lack of measurement data and the newly growing awareness of the phenomenon's existence. Studies on SubUHI have been performed in many parts of the world. This phenomenon, known as the Subsurface Urban Heat Island, refers to elevated temperatures in soil [6,7] or groundwater [8,9]. The higher groundwater temperature in urban areas is defined as a Groundwater Urban Heat Island (GUHI) [10]. A significant amount of research on SubUHI focuses on assessing the geothermal energy potential in urban areas [11,12], driven by the increasing demand for energy and heightened ecological awareness. The identification of the Subsurface Urban Heat Island has been carried out through both satellite techniques [13,14] and in-situ measurements [15,16]. Satellite-derived land surface temperature (LST) is also used to study UHI. This is an innovative remote sensing method for measuring above-ground temperatures. While it suggests a correlation with air and ground surface temperatures, the exact relationships are not yet fully defined [17,18]. Nonetheless, satellite-derived Land Surface Temperature (LST) provides convenient access to both the spatial and temporal characteristics of Urban Heat Islands (UHIs).

Urban regions are increasingly experiencing subsurface heat islands, a phenomenon linked to underground climate change that contributes to environmental issues, public health challenges, and transportation disruptions. This warming of urban soil arises from both human activities and weather-related factors [19]. SubUHI poses environmental concerns due to its impact on groundwater quality, affecting its chemical, physical, and biological properties [20], as well as on living ecosystems [21].
Studies on subsurface temperatures have been conducted in many countries around the world, including: Germany [8,16,22], Switzerland [3], Czech Republic [23,24], Italy [9,25,26], Spain [27], France [28], United Kingdom [29], Netherlands [30], USA [23,31], Canada [15], Japan [32–35], South Korea, Thailand [33,34]. Each of the above-mentioned studies confirms the warming of subsurface areas. Studies in Asia have shown that the subsurface warming in the analysed cities ranges between 1.8 °C and 2.8 °C [33]. Studies focusing on the relationship between air temperature and ground temperature show that there is a relationship between them and based on meteorological information, annual differences between temperatures can be estimated [23]. The conducted groundwater temperature (GWT) measurements allowed the determination of the increase in GWT over time. According to Memberg et al. [22], for the area of cities in Germany (Berlin, Munich, Frankfurt, Karlsruhe, Cologne, Darmstadt) the SubUHI intensity ranges from 1.9 to 2.4 K, while according to Zhu et al. [16], for Cologne alone the groundwater temperature for the city center increased by 5K. For the Paris area the GWT in the last century increased on average by 0.9 °C [28], for Amsterdam 4.1 °C [30] and 3.5 °C for Istanbul [36]. On the other hand, for the Basel area it was defined that the GWT is higher by 5 °C than the average air temperature [3], and studies carried out for Milan revealed differences of up to 3 °C in GWT between the city center and the surrounding rural areas [9]. The above studies have shown an increase in the temperature beneath the city surface in various parts of the world by 2-8 °C. In these studies, temperature-depth profiles are often used, which allow determining temperature changes over time and depth [32–34,37]. GWT data are compared with the city's land cover and meteorological data to determine the relationship between temperatures [16,26]. To investigate the SubUHI phenomenon, 3D city models and time series analyses were utilized [9,16,25]. It has been established that the temperature below the earth's surface is influenced by: solar radiation, air temperature, wind speed, rainfall, shelter, and soil properties [38]. It is recognized that several natural and human-related factors influence the thermal regime of groundwater: the thickness of the unsaturated zone, the speed of

groundwater flow, the presence of surface water reservoirs and the degree of interaction with groundwater, the percentage of buildings and artificial areas, and the presence of underground infrastructure [8,11,39]. At the same time, studies have shown that global warming contributes to the increase in groundwater temperatures [33]. Additionally, research has revealed a correlation between climatic conditions and the temperature of shallow surface waters [26].

Research on GWT for Wrocław was first conducted by Worsa-Kozak et al. [10] in 2004-2005 and by Buczyński et al. [40] in 2011-2012. These studies were limited to temperature measurements without depth profiles and analyzed only the GWT and air relationships without incorporating spatial distribution analyses or spatial statistics. For the period 2004-2005 the lowest monthly average GWT of 8.64 °C was recorded in March 2005 and the highest of 16.92 °C in August 2004. In 2011-2012, the average water temperature in the tested points was 11.7°C. The lowest temperature of 6.5°C was recorded in the points located in the north-eastern part of the city, while the highest was 17.1°C in the city centre. These studies confirm that elevated groundwater temperatures are observed in the center of the city of Wrocław. Additionally, the authors of both works indicate a time shift between air temperature and GWT of about 5-6 weeks for data from the years 2004-2005 and 3-4 months for the years 2011-2012 but both studies were performed using different methods.

Thus, the main objective of our study is to analyse groundwater temperature in Wroclaw based on 2 years of measurements including the spatial context of GWT and the relationship between ambient air temperature and groundwater temperature. In addition, our study aimed at analysis of groundwater temperature change with depth separately for Quaternary and Tertiary aquifers.

2. STUDY AREA

Wroclaw is the capital of the Lower Silesia region in SW Poland and the third largest city in Poland with population estimated in 2024 at approx. 673 500 inhabitants and area of 292.8 km² [41]. The city stretches for over 26 km from east to west and over 19 km from north to south and is situated along the Oder River and its four tributaries, which flow into it within the city's limits. These are: Bystrzyca, Oława, Ślęza, and Widawa rivers.

Most of the city is located within the Fore-Sudetic Monocline, but its south-western edges are located within an older unit called the Fore-Sudetic Block. Both structures are separated by two dislocation systems characterised by parallel and perpendicular faults, with a common name: the Middle Odra Fault Zone [42,43]. These faults are of a throwing nature, and the displacements of the blocks relative to each other amount to several hundred meters. The Fore-Sudetic Monocline and the Fore-Sudetic Block and the dislocations separating them are covered by Cenozoic sediments. The geology in the Wrocław area is shown in Fig. 1. There are four main aquifers [44]. The youngest of them is the Holocene-Pleistocene (also called the Quaternary), which is composed of sandy-gravel sediments of fluvioglacial and fluvial origin. Below, there are poorly permeable or only locally permeable Miocene formations (the Tertiary, also called the Paleogene-Neogene). The older, Mesozoic aquifer is composed of fissure and fissure-karst rocks formed in the Triassic. In turn, the lowest and least explored aquifer structure is the Permian [45]. The first groundwater table is located at a depth of 2 to 8 m below ground level and is mainly unconfined. In the Odra River Valley area, the first aquifer is continuous and unconfined and the groundwater table is usually below 5 m [45].

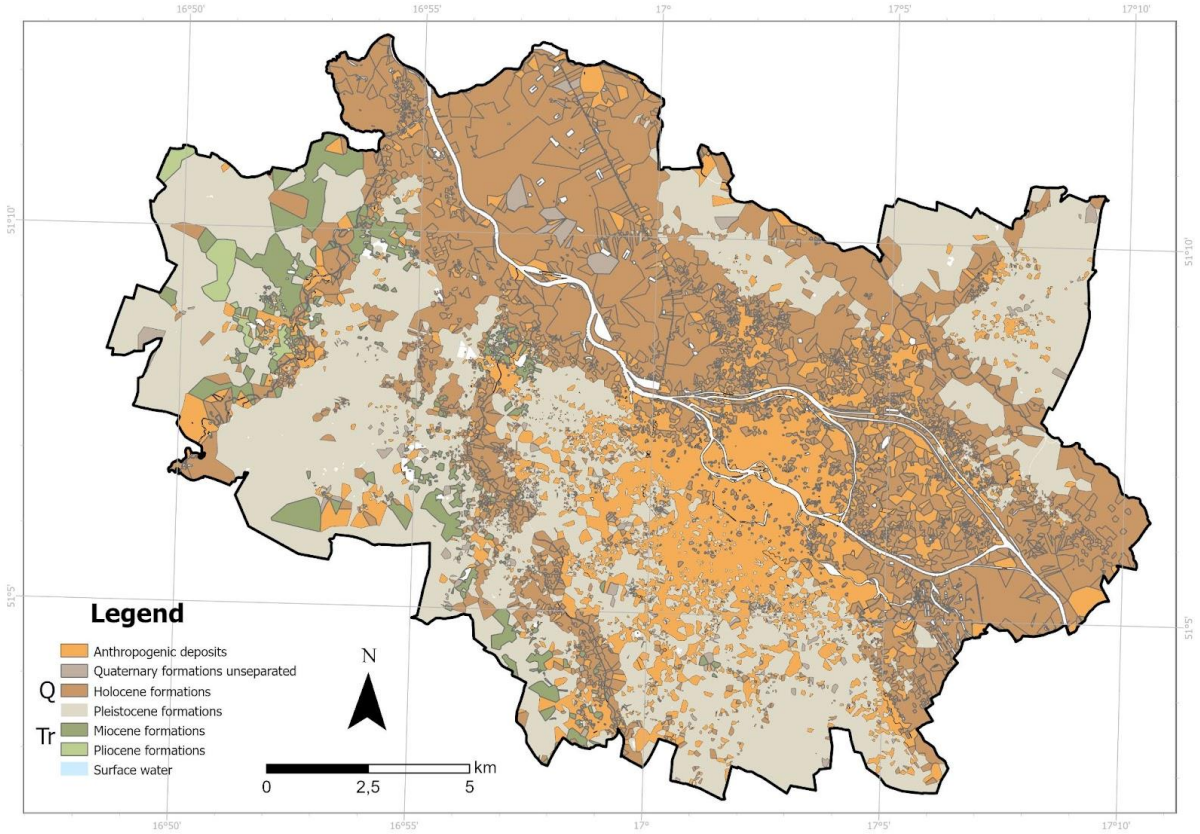

Fig. 1. Geological structure of Wrocław at a depth of 1 meter below the ground surface (compiled using data from: https://baza.pgi.gov.pl)

34% of the city area is occupied by green areas, 25% by agricultural areas, while residential, economic and service areas account for approx. 23% [46]. Built-up areas are mainly concentrated in the center, south and north-west of the city. The highest density of green areas is located in the peripheral zone (Fig. 2). The natural axis of the city is the Odra River, which is the second largest river in Poland. Wrocław is located in the upper part of the middle Odra [47]. The Odra within Wrocław is 26 km long and flows from the south-east to the north-west. The total length of watercourses in the city is 280 km [48]. The city is characterized by a typical transitional climate of the temperate zone. Oceanic and continental influences determine the diversity of weather conditions. The average annual air temperature in Wrocław is 9.0°C, in the coldest month (January) -0.4°C, and for the warmest month (July) 18.8°C. The annual temperature amplitude is 19.2°C. In the 2008-2019 period the average annual air temperature was 10.2 °C [30]. Precipitation in Wrocław occurs on 167 days a year, while the average annual precipitation sum from the 1901–2000 period is 583 mm [49].

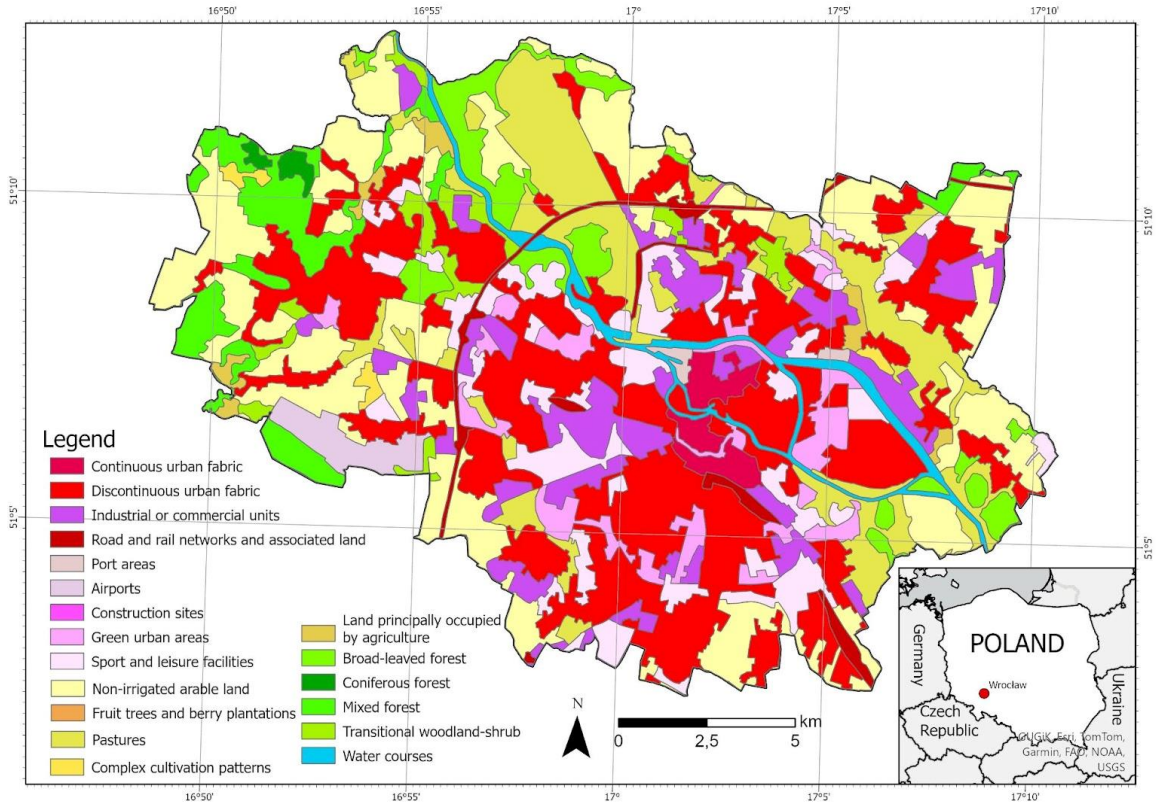

Fig. 2. Main land cover types in Wroclaw based on the Corine Land Cover database from 2018. (compiled using data from: https://clc.gios.gov.pl)

3. MATERIALS AND METHODOLOGY

Our study composed of the following phases: dentification of available wells for groundwater temperature readings, observation of temperature at set intervals and development of geodatabase of measurements, and statistical analysis of results.

3.1. Measurement technique

The measurements of groundwater parameters in the shallowest aquifer layer in Wrocław were carried out from June 2022 to June 2024 in a monitoring network consisting of 19 wells. 8 of these wells were drilled in Tertiary formations and 11 in Quaternary deposits. The readings of groundwater table depth, temperature and conductivity were taken twice a month. Temperature and conductivity were recorded in 1 m intervals up to a depth of 17 m below the ground surface. We used the Solinst Model 107 electronic probe attached to a PVDF tape with a temperature range of -15 ˚C to +50 ˚C, and measurement accuracy of ± 0.2 ˚C. The conductivity range of the device is 0-80,000 µS/cm with 5% accuracy [50]. In this study, we concentrated on the analysis of groundwater temperature. The location of measurement points is shown in Figure 3, and a representative point with the Solinst 107 TLC Meter is presented in Figure 4.

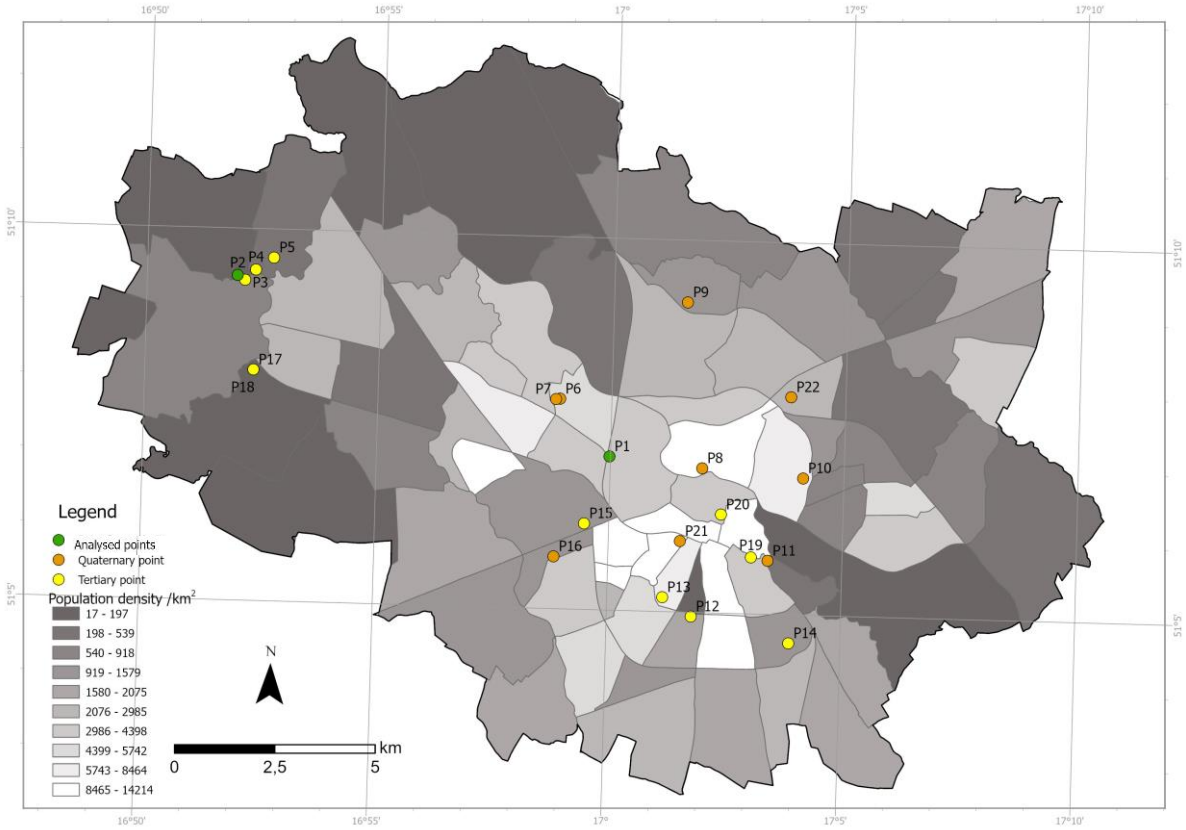

Fig. 3. Map of measurement points and population density for the study area (compiled using data from: https://geoportal.wroclaw.pl/)

Fig. 4. The top of a measurement point and the measuring device Solinist 107TLC

3.2. Statistical analysis of measurement data

We have used basic statistical measures, such as mean, max., min., and standard deviation, to describe and summarize the properties of the recorded set temperature readings. The results have been presented in tables and graphs, as well as temperature profiles. In addition, we have used the Inverse Distance Weighted (IDW) interpolation method to obtain the spatial distribution of temperature measured at 1 m below the groundwater table as a continuous field. The results have been graphically presented as isolines with 0.5 ˚C intervals. We developed maps for the winter (cold, from November to April) and summer (warm, from May to October) half-years and for the full hydrological years. The IDW is a deterministic method for multivariate interpolation with a known scattered set of points. The assigned values to unknown points are calculated with a weighted average of the values at the known points [51]. We created the groundwater temperature maps for IDW parameters optimized with a cross-validation technique [52]. The weight parameter values ranged from 1 to 2 for the hydrological year and summer 2022 maps and winter 2023/2024 maps, respectively. The RMS values for the interpolation results ranged from 2.83 °C for the winter 2023/2024 map to 3.15 °C for the summer 2023 map. The results were analysed in two ways: in terms of the period of groundwater origin and in terms of the depth of their occurrence. For each of the groups, exploratory data analysis was performed. Measurements taken 1 meter below the ground water level were used for further analyses.

4. RESULTS

The mean water temperature for all points throughout the measurement period was 12.7 °C, ranging from 8.9 to 25.4 °C. The lowest temperature was recorded slightly to the south-east of the city centre, while the highest temperature was recorded at the piezometer in the city center. However, the lowest average temperature for the entire period was noted at points in the western part of the city, while the highest was in the center. For the defined measurement periods, in the hydrological year 2022/2023, the minimum GWT value was 9.2 °C, the maximum 25.4 °C, and the average 12.8 °C. In the warm periods, these parameters had the following values: 9.9 °C, from 25.1 °C to 25.4 °C and from 12.9 °C to 13.3 °C respectively, while for the cold period, from 8.9 °C to 9.2 °C, from 23.6 °C to 24.4 °C and from 12.2 °C to 12.3 °C respectively. The standard deviation in the entire measurement period ranges between 3 °C and 3.7 °C. Basic statistics calculated from the measurement results for the analysed periods (hydrological year, summer, and winter) are presented in Table 1.

Table 1. Descriptive statistics for measurement data

Period	Min. [°C]	Max. [°C]	Mean [°C]	Std. Dev. [°C]
Hydrological year 2022/2023	9.2	25.4	12.8	3.2
Summer 2022	9.9	25.1	13.3	3.5
Winter 2022/2023	9.2	23.6	12.3	3.0
Summer 2023	9.9	25.4	12.9	3.3
Winter 2023/2024	8.9	24.4	12.2	2.5

For measurement data recorded at 1 meter below the water table, further statistical analyses were performed. The data set was divided into points representing aquifers in Tertiary and Quaternary

formations. These data were compared with air temperature. The results are presented in Fig. 5 and Fig. 6. The measurement results for the Tertiary show little variability in time, their values are at a similar level throughout the measurement period. The values recorded in Quaternary wells vary in time and are characterized by seasonality. A trend in the behaviour of GWT for Quaternary aquifers similar to air temperature can be observed. The time shift between these two data sets was detected with the GWT delayed by about 4-8 weeks in relation to air temperature.

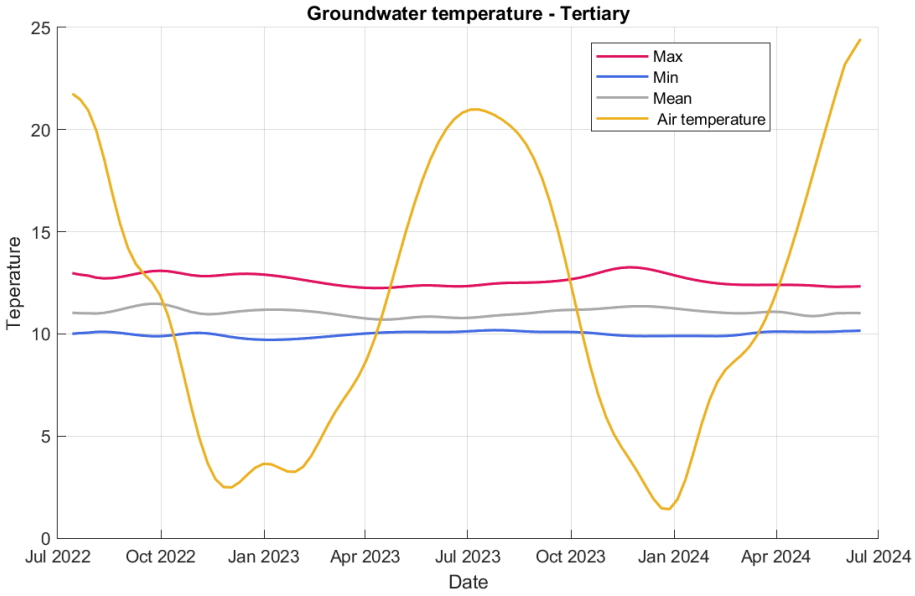

Fig. 5. Temporal trajectory of the groundwater and ambient air temperatures in the study area - measurement points of GWT in Tertiary aquifer

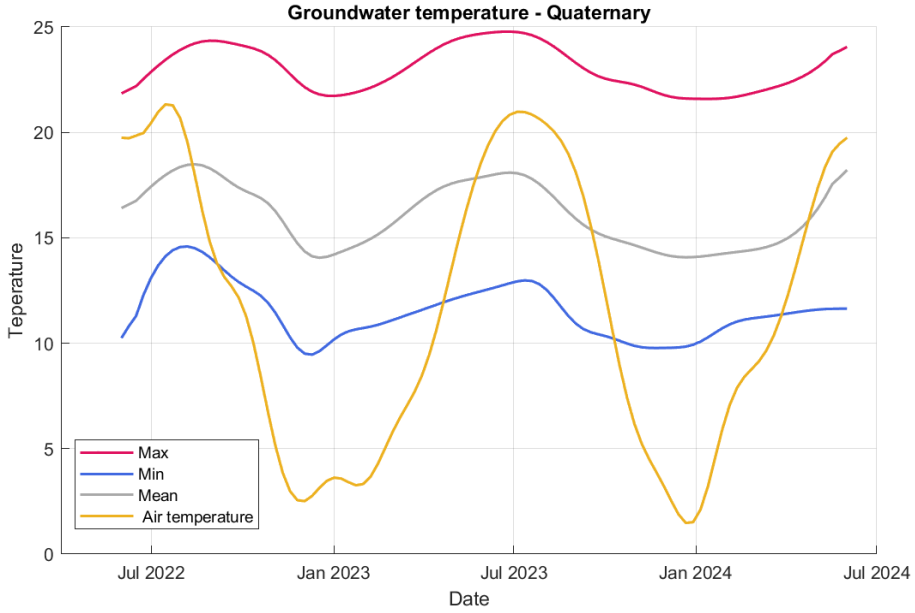

Fig. 6. Temporal trajectory of the groundwater and ambient air temperatures in the study area - measurement points of GWT in Quaternary aquifer

To illustrate changes in water temperature with depth below the ground level, graphs were prepared showing temperature readings at different depths for the hydrological year (Fig. 8), warm season (summer) (Fig. 9) and cold season (winter) (Fig. 10). The graphs show that in most measurement points, the temperature decreases as depth increases. However, there are points where this process is the opposite - the temperature increases with depth. This is the case for the warmest point - winter (Fig. 10). At smaller depths, the water temperature varies more, which may suggest the influence of external factors. For all analysed periods, the highest temperatures >20°C occur at one point, so it is necessary to look for additional factors causing this anomaly. At greater depths of approx. 15 meters, the temperature profiles become stable. Thus, our results confirm that at depths of approx. 15 meters the influence of external factors on GWT disappears. The graphs emphasize the importance of local conditions in shaping groundwater temperatures. Points showing similar profiles may be characterized by similar geological or hydrogeological conditions in their vicinity. Comparing the graphs in Fig. 9 and 10, it can be seen that the temperature variability depending on the depth in the summer period is much greater than in the winter period.

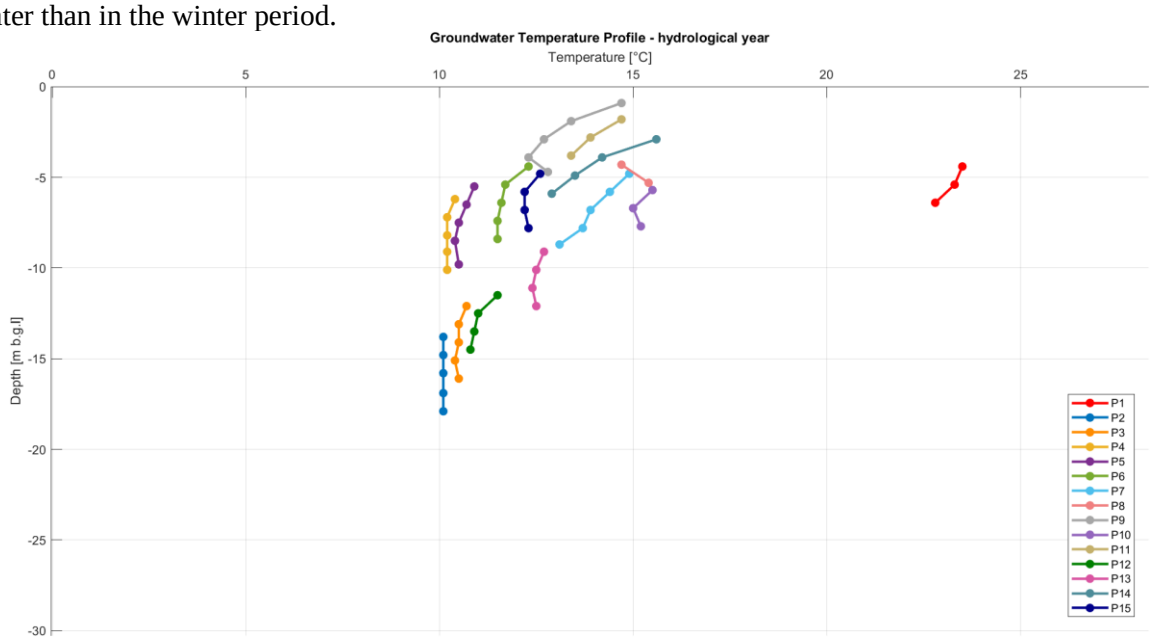

Fig. 7 Groundwater temperature profile - hydrological year

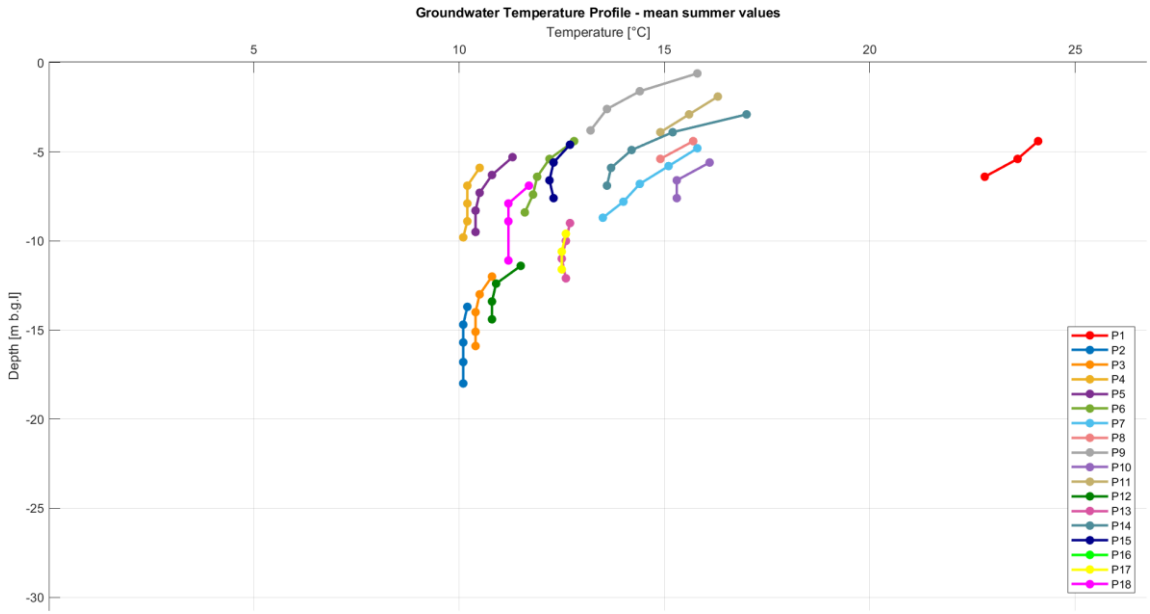

Fig. 8 Groundwater temperature profile - summer period

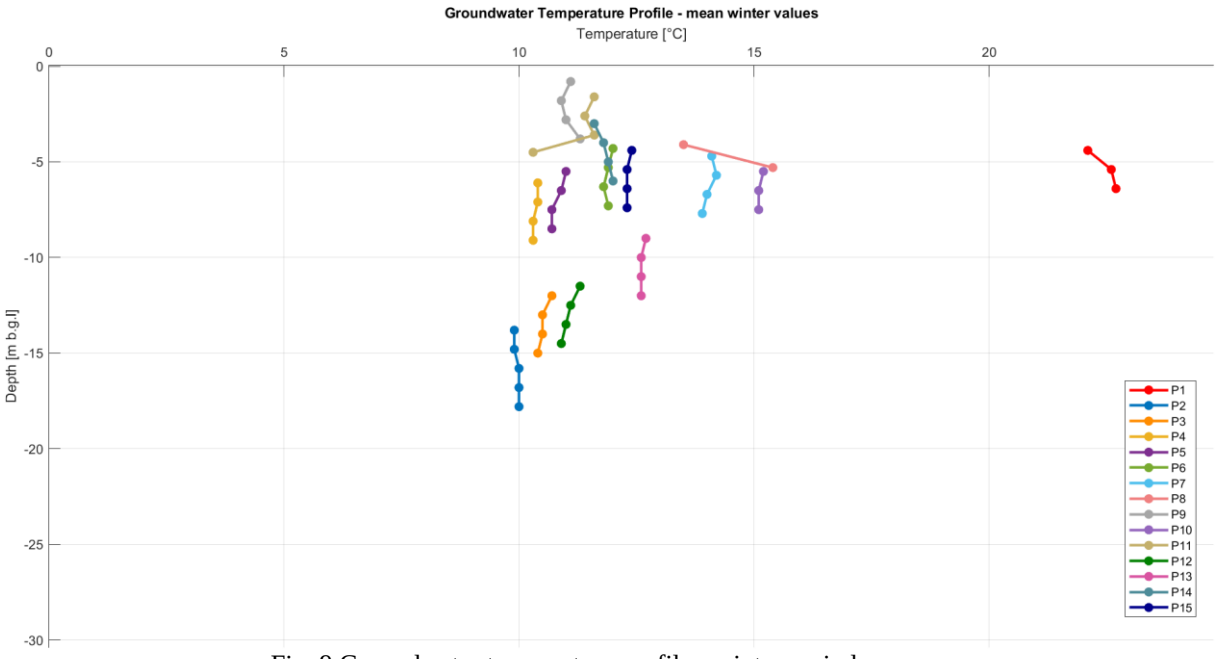

Fig. 9 Groundwater temperature profile - winter period

Analysing seasonal thermal gradient for the two geological formations, it can be concluded that the thermal gradient for the Tertiary is relatively low and stable over time. The values range from -0.17 °C/m (the greatest variability in summer 2022) to -0.01 °C/m (the minimum variability in winter 2023/2024). This indicates that these aquifers are less susceptible to seasonal temperature changes. In the case of the Quaternary aquifer water, the gradient is more variable and depends on the season. The most remarkable differences were recorded in summer 2022 (-1.17 °C/m), indicating a strong influence

of seasonal temperature changes on this aquifer. In winter 2022/2023 (-0.01 °C/m), the gradient almost disappears, which means that this layer reaches relative thermal equilibrium at this time and the temperature differences with depth are minimal.

Tab. 2. Thermal gradient for analysed periods

Thermal gradient [°C/m]		
Period	**Tertiary**	**Quaternary**
Hydrological year 2022/2023	-0.15	-0.32
Summer 2022	-0.17	-1.17
Winter 2022/2023	-0.06	-0.01
Summer 2023	-0.16	-0.44
Winter 2023/2024	-0.01	0.05

Looking at the spatial distribution of GWT 1 m below the water table (Fig. 10, Fig. 11), higher values are clearly visible in the city centre, while the lowest in the western part of the city. In the warm period, a larger area of the city is characterised by increased (higher than mean) GWT values than in the cold period. In both of these periods, lower groundwater temperatures occur on the outskirts of the city. In the cold periods, GWT values range from 9 °C to 12 °C across a significant portion of the city, particularly in the western part. Due to the lack of a measurement point in the north-eastern part of the city, the presented spatial distribution may be susceptible to error. The annual map (Fig. 10) and seasonal maps (Fig. 11) indicate an evident influence of climatic and seasonal changes on groundwater temperature. The eastern and central parts of the area are warmer most of the year. The western regions are cooler, suggesting deeper water sources or a greater influence of a colder local climate. The apparent differences between seasons (especially summer/winter) show the influence of seasonal heating and cooling.

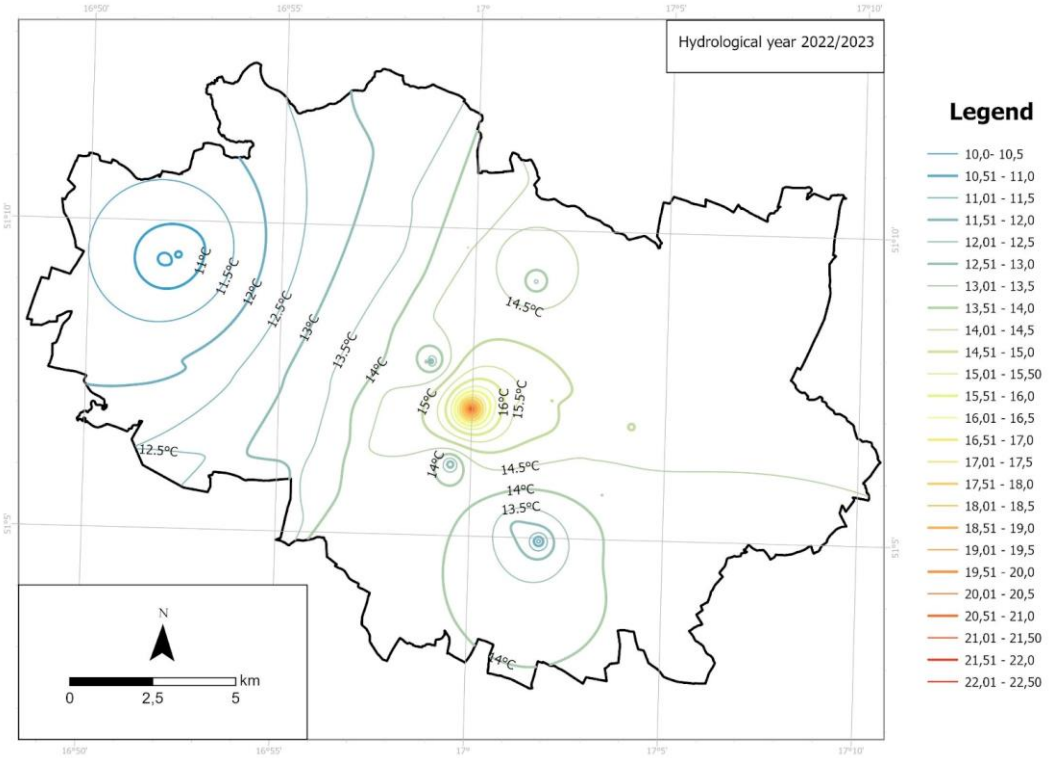

Fig. 10. Spatial distribution map of GWT – hydrological year 2022/2023

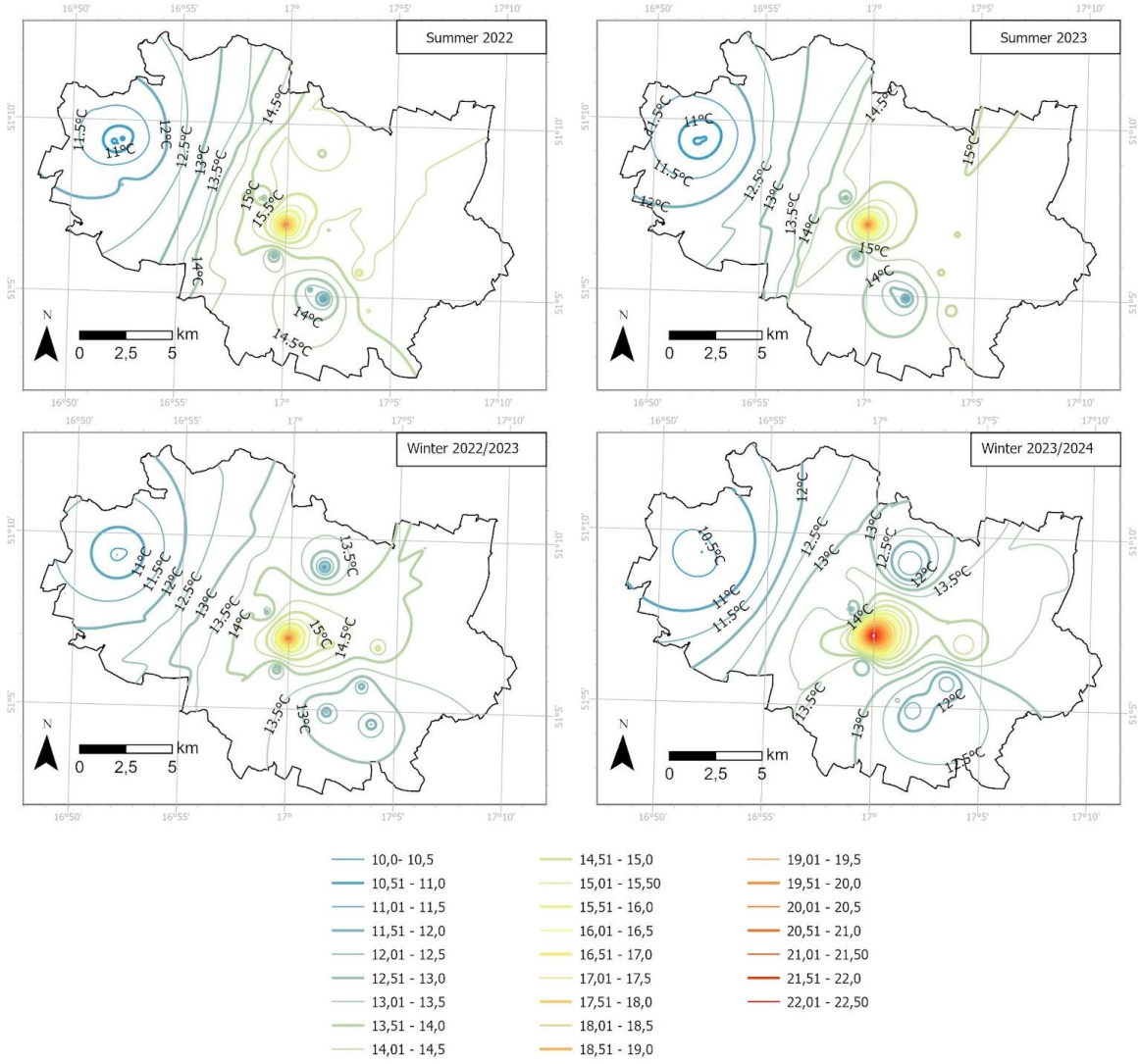

Fig. 11. Spatial distribution map of GWT – seasonal data for 2022/2024

We have additionally analysed 2 selected points, the warmest (P1) and the coldest (P2). Their location is shown in Fig. 3. The coldest point is characterized by a temperature ranging from 9.7 °C to 10.8 °C. The greatest depth at which the measurement took place was 18.18 m and the GWT value was 10.1 °C. This point is located on the outskirts of the city in a green area. For the warmest point located in the city center, the GWT value range was between 19.6 °C and 25.4 °C. The deepest measurement was taken at 6.62 m below ground level and the temperature reading was 22.7 °C. The indicated point is located in a grassy area, but there are many areas covered with artificial surfaces, a busy road and a heating network in its vicinity. We have found that due to the underground infrastructure, the GWT values for this point reach significantly higher values than at other measurement points. This clearly indicates local anomalies caused by technical infrastructure used for heat transfer.

5. DISCUSSION

In this paper, an analysis of groundwater temperature measurements for Wrocław in the period 2022-2024 was carried out. The results presented in this paper are consistent with previous studies conducted in other cities worldwide, which confirm the increase in temperatures in the subsurface zones [16,28,30,33]. The demonstrated groundwater temperature values for Wrocław (average 12.7 °C, maximum 25.4 °C) and differences between warm and cold periods of the year indicate a significant influence of both natural and anthropogenic factors on the thermal conditions of the underground environment, which should be taken into account in further considerations. Many factors can affect groundwater temperature variability, including seasonal changes. The results of the study in Wrocław revealed clear seasonal fluctuations, with higher groundwater temperatures recorded in warmer periods. This is consistent with the work of [53] who confirm that groundwater temperatures in urban areas show a delayed but correlated response to the surface air temperature.

The spatial distribution of GWT in Wrocław is similar to those obtained in other European cities [8,22,25,30]. The highest values of groundwater temperature are located in the city center and gradually decrease with distance from the center. This observation is consistent with findings from Benz et al. [8], who analysed urban subsurface warming in several German cities, including Cologne. In Wrocław, with a population density of approximately 2200 inhabitants per square kilometer (based on 2022 data) [41], the average groundwater temperature was 12.7 °C, with a maximum of 25.4 °C recorded in central areas. This is comparable to Cologne, where observed a mean groundwater temperature with values 12.4 °C in high-density areas (population density: approximately 2500 inhabitants per square kilometer). Compared to previous studies for Wrocław, which were conducted for the years 2004–2005 [10] and 2011–2012 [40], the current results indicate a continuation of the rising trend in groundwater temperatures. It should be noted that due to the character of the studied environment, all of these studies are probably subjected to error resulting from the short period of observation, low frequency of measurements, limited number of measurement points, and their uneven distribution across the city.

6. CONCLUSION

In this article, descriptive statistics for groundwater temperature in Wrocław based on two years of measurements were presented. These results allowed us to characterise the changes in GWT with location and depth. Our studies confirmed that water temperature is higher in the city centre compared to the outskirts and the occurrence of seasonal changes in groundwater temperature in Wrocław. The time shift between changes in air temperature and groundwater temperature was determined to be from approx. 4 to 8 weeks for Wroclaw. The spatial distribution of GWT and local temperature anomalies may also be influenced by the underground technical infrastructure, as shown in the case study of one of the measurement points. Therefore, further analyses of measurements should be carried out, taking into account the underground technical infrastructure. The collected data, in comparison to results presented in publications by other authors [10,40], provide a description of GWT changes in Wrocław over the last 20 years and confirm changes below the ground level that are probably associated with urban development and climate change. Our results confirm also that the influence of external factors on the temperature of underground water is transferred to a depth of approximately 15 meters.

REFERENCES

1. United Nations Department of Economic and Social Affairs 2019, World Urbanization Prospects: The 2018 Revision (UN). Available online. Access: 2024-12-03.
2. Yu, Z, Yao, Y, Yang, G, Wang, X and Vejre, H 2019. Strong contribution of rapid urbanization and urban agglomeration development to regional thermal environment dynamics and evolution. F*orest Ecology and Management*, **446**, 214–25.
3. Epting, J and Huggenberger, P 2013. Unraveling the heat island effect observed in urban groundwater bodies – Definition of a potential natural state. *Journal of Hydrology* **501**, 193–204
4. Oke, TR 1982. The energetic basis of the urban heat island. J*ournal of the Royal Meteorological Society*, 1–24.
5. Oke, TR 1995. The Heat Island of the Urban Boundary Layer: Characteristics, Causes and Effects Wind Climate in Cities. ed J E Cermak, A G Davenport, E J Plate and D X Viegas (Dordrecht: Springer Netherlands), pp 81–107.
6. Vasenev, V, Varentsov, M, Konstantinov, P, Romzaykina, O, Kanareykina, I, Dvornikov, Y and Manukyan, V 2021. Projecting urban heat island effect on the spatial-temporal variation of microbial respiration in urban soils of Moscow megalopolis. *Science of The Total Environment* **786**, 147457.
7. Edmondson, JL, Stott, I, Davies, ZG, Gaston, KJ and Leake, JR 2016. Soil surface temperatures reveal moderation of the urban heat island effect by trees and shrubs. *Sci Rep* **6**, 33708.
8. Benz, SA, Bayer, P, Menberg, K, Jung, S and Blum, P 2015. Spatial resolution of anthropogenic heat fluxes into urban aquifers. *Science of The Total Environment* **524–525**, 427–439.
9. Previati, A and Crosta, GB 2021. Characterization of the subsurface urban heat island and its sources in the Milan city area, Italy. *Hydrogeol J* **29**, 2487–500.
10. Worsa-Kozak, M and Arsen, A 2023. Groundwater Urban Heat Island in Wrocław, Poland. *Land* **12**, 658.
11. Menberg, K, Blum, P, Schaffitel, A and Bayer, P 2013. Long-Term Evolution of Anthropogenic Heat Fluxes into a Subsurface Urban Heat Island. *Environ. Sci. Technol.* **47**, 9747–55.
12. Luo, Z and Asproudi, C 2015. Subsurface urban heat island and its effects on horizontal ground-source heat pump potential under climate change. *Applied Thermal Engineering* **90**, 530–7.
13. Zhan, W, Ju, W, Hai, S, Ferguson, G, Quan, J, Tang, C, Guo, Z and Kong, F 2014. Satellite-Derived Subsurface Urban Heat Island. *Environ. Sci. Technol.* **48**, 12134–40.
14. Huang, S, Pollack, HN and Shen, P-Y 2000. Temperature trends over the past five centuries reconstructed from borehole temperatures. *Nature* **403**, 756–8.
15. Ferguson, G and Woodbury, A D 2007. Urban heat island in the subsurface: Subsurface urban heat island. *Geophys. Res. Lett*. **34.**
16 Zhu, K, Bayer P, Grathwohl, P and Blum, P 2015. Groundwater temperature evolution in the subsurface urban heat island of Cologne, Germany. *Hydrol. Process*. **29**, 965–78.
17. Hachem, S, Duguay, CR and Allard, M 2012. Comparison of MODIS-derived land surface temperatures with ground surface and air temperature measurements in continuous permafrost terrain. *The Cryosphere* **6**, 51–69.
18. Schwarz, N, Schlink, U, Franck, U and Großmann, K 2012. Relationship of land surface and air temperatures and its implications for quantifying urban heat island indicators—An application for the city of Leipzig (Germany). *Ecological Indicators* **18**, 693–704.
19. Rotta Loria, AF 2023. The silent impact of underground climate change on civil infrastructure. *Commun Eng* **2**, 44.

20. Blum, P, Menberg, K, Koch, F, Benz, SA, Tissen, C, Hemmerle, H and Bayer, P 2021. Is thermal use of groundwater a pollution? *Journal of Contaminant Hydrology* **239**, 103791.
21. Brielmann, H, Griebler, C, Schmidt, SI, Michel, R and Lueders, T 2009. Effects of thermal energy discharge on shallow groundwater ecosystems: Ecosystem impacts of groundwater heat discharge FEMS Microbiology. *Ecology* **68**, 273–86.
22. Menberg, K, Bayer, P, Zosseder, K, Rumohr, S and Blum, P 2013. Subsurface urban heat islands in German cities. *Science of The Total Environment* **442**, 123–33.
23. Smerdon, JE, Pollack, HN, Cermak, V, Enz, JW, Kresl, M, Safanda, J and Wehmiller, JF 2006. Daily, seasonal, and annual relationships between air and subsurface temperatures. *J. Geophys. Res*. **111**.
24. Čermák, V, Bodri, L, Šafanda, J, Krešl, M and Dědeček, P 2014. Ground-air temperature tracking and multi-year cycles in the subsurface temperature time series at geothermal climate-change observatory. *Stud Geophys Geod* **58**, 403–24.
25. Previati, A, Epting, J and Crosta, GB 2022. The subsurface urban heat island in Milan (Italy) - A modeling approach covering present and future thermal effects on groundwater regimes. *Science of The Total Environment* **810**, 152119.
26. Bucci, A, Barbero, D, Lasagna, M, Forno, MG and De Luca, DA 2017. Shallow groundwater temperature in the Turin area (NW Italy): vertical distribution and anthropogenic effects. *Environ Earth Sci* **76**, 221.
27. García-Gil, A, Vázquez-Suñe, E, Schneide, EG, Sánchez-Navarro, JÁ and Mateo-Lázaro, J 2014. The thermal consequences of river-level variations in an urban groundwater body highly affected by groundwater heat pumps. *Science of The Total Environment* **485–486**, 575–87.
28. Perrier, F, Le Mouël, J-L, Poirier, J-P and Shnirman, M G 2005. Long-term climate change and surface versus underground temperature measurements in Paris. *Int. J. Climatol*. **25**, 1619–31.
29. Farr, GJ, Patton, AM, Boon, DP, James, DR, Williams, B and Schofield, DI 2017. Mapping shallow urban groundwater temperatures, a case study from Cardiff, UK. *Quarterly Journal of Engineering Geology and Hydrogeology* **50**, 187–98.
30. Visser, P W, Kooi, H, Bense, V and Boerma, E 2020. Impacts of progressive urban expansion on subsurface temperatures in the city of Amsterdam (The Netherlands). *Hydrogeol J* **28**, 1755–72.
31. Rotta Loria, AF, Thota, A, Thomas, AM, Friedle, N, Lautenberg, JM and Song, EC 2022. Subsurface heat island across the Chicago Loop district: Analysis of localized drivers. *Urban Climate* **44**, 101211.
32. Taniguchi, M and Uemura, T 2005. Effects of urbanization and groundwater flow on the subsurface temperature in Osaka, Japan. *Physics of the Earth and Planetary Interiors* **152**, 305–13.
33. Taniguchi, M, Uemura, T and Jago-on, K 2007. Combined Effects of Urbanization and Global Warming on Subsurface Temperature in Four Asian Cities. *Vadose Zone Journal* **6**, 591–6.
34. Yamano, M, Goto, S, Miyakoshi, A, Hamamoto, H, Lubis, RF, Monyrath, V and Taniguchi, M 2009. Reconstruction of the thermal environment evolution in urban areas from underground temperature distribution. *Science of The Total Environment* **407**, 3120–8.
35. Huang, S, Taniguchi, M, Yamano, M and Wang, C 2009. Detecting urbanization effects on surface and subsurface thermal environment — A case study of Osaka. *Science of The Total Environment* **407**, 3142–52.
36. Yalcin, T and Yetemen, O 2009. Local warming of groundwaters caused by the urban heat island effect in Istanbul, Turkey. *Hydrogeol J* **17**, 1247–55.
37. Salem, Z E-S and Osman, OM 2016. Shallow subsurface temperature in the environs of El-Nubaria canal, northwestern Nile Delta of Egypt: implications for monitoring groundwater flow system. *Environ Earth Sci*. **75**, 1241.

38. Liu, C, Shi, B, Tang, C and Gao, L 2011. A numerical and field investigation of underground temperatures under Urban Heat Island. *Building and Environment* **46**, 1205–10.
39. Ferguson, G and Woodbury, A D 2004. Subsurface heat flow in an urban environment. *J. Geophys. Res.* **109**, 2003JB002715.
40. Buczyński, S and Staśko, S 2013. Temperatura płytkich wód podziemnych na terenie Wrocławia [The temperature of shallow groundwater in the Wrocław area]. *Biuletyn Państwowego Instytutu Geologicznego* **456**, 51–5.
41. Główny Urząd Statystyczny - wroclaw.stat.gov.pl [Statistics Poland] Available online. Access: 2024-12-03.
42. Winnicka, G 1988. Objaśnienia do szczegółowej mapy geologicznej Polski 1:50000. [Explanations for the detailed geological map of Poland]. Wydawnictwo Geologiczne.
43. Różycki, M 1968; Budowa geologiczna okolic Wrocławia. [Geological structure of the Wrocław area], *Biul. Inst. Geologicznego* **214**.
44. Malinowski, J 1991. Budowa geologiczna Polski. [Geological structure of Poland]. *Hydrogeologia 7*. Warszawa: Wyd. Geol.
45. Mądrala, M 2002. Budowa geologiczna i wody podziemne okolic Wrocławia. [Geological structure and underground waters of the Wrocław area]. Raport 2002 – Środowisko.
46. Wroclaw City Council. Study of the Conditions and Directions of Spatial Development in Wrocław; Wroclaw City Council: Wroclaw, Poland, 2018. (In Polish).
47. Bożek, A, Dubicki, A, Dziewanowski, M, Kwiatkowska-Szygulska, B 2002. Wody powierzchniowe. [Surface water]. Środowisko Wrocławia – Informator 2002, Dolnośląska Fundacja Ekorozwoju, Wrocław.
48. Goldsztejn, J, Frankowski, Z, Badura, J and Tarnawski, M 2009. Baza danych geologiczno-inżynierskich wraz z opracowaniem Atlasu geologiczno – inżynierskiego aglomeracji wrocławskiej. [Database of geological and engineering databases, including the Geological and Engineering Atlas of the Wrocław Agglomeration], Wrocław.
49. Dubicki, A, Dubicka, M and Szymanowski, M 2002. Klimat Wrocławia. [The climate of Wrocław]. Available online. Access: 2024-12-03.
50. Solnist - https://www.solinst.com/ Access: 2024-12-03.
51. Tomczak, M 1998. Spatial interpolation and its unceratinty using automated anistropic inverse distance weighting (IDW) - cross-validation/jackknife approach. *Journal of Geographic Information and Decision Analysis* **2**, 18-30.
52. Hofierka, J, Cebecauer, T and Šúri, M 2007. Optimisation of Interpolation Parameters Using Cross-validation Digital Terrain Modelling. *Lecture Notes in Geoinformation and Cartography* ed R J Peckham and G Jordan (Berlin, Heidelberg: Springer Berlin Heidelberg), 67–82.
53. Taylor, CA and Stefan, HG 2009. Shallow groundwater temperature response to climate change and urbanization. *Journal of Hydrology* **375**, 601–12.